Proc. Natl. Acad. Sci. USA
Vol. 94, pp. 10183–10188, September 1997
Cell Biology

Inhibition of Reaper-induced apoptosis by interaction with inhibitor of apoptosis proteins (IAPs)

DOMAGOJ VUCIC*, WILLIAM J. KAISER*, ALEX J. HARVEY*, AND LOIS K. MILLER*†‡

Departments of *Genetics and †Entomology, University of Georgia, Athens, GA 30602

Contributed by Lois K. Miller, July 15, 1997

ABSTRACT **IAPs comprise a family of inhibitors of apoptosis found in viruses and animals. *In vivo* binding studies demonstrated that both baculovirus and *Drosophila* IAPs physically interact with an apoptosis-inducing protein of *Drosophila*, Reaper (RPR), through their baculovirus IAP repeat (BIR) region. Expression of IAPs blocked RPR-induced apoptosis and resulted in the accumulation of RPR in punctate perinuclear locations which coincided with IAP localization. When expressed alone, RPR rapidly disappeared from the cells undergoing RPR-induced apoptosis. Expression of P35, a caspase inhibitor, also blocked RPR-induced apoptosis and delayed RPR decline, but RPR remained cytoplasmic in its location. Mutational analysis of RPR demonstrated that caspases were not directly responsible for RPR disappearance. The physical interaction of IAPs with RPR provides a molecular mechanism for IAP inhibition of RPR's apoptotic activity.**

Apoptosis, or programmed cell death, plays a major role in development and homeostasis in vertebrates and invertebrates (1), and the improper control of apoptosis contributes to the progression of a number of human diseases (2). In *Drosophila*, ectopic expression of *rpr*, which encodes a 65-amino acid peptide (Reaper; RPR), induces death in cells in which it is expressed (3, 4), and induction of expression of an exogenous copy of *rpr* in a *Drosophila* cell line results in rapid death accompanied by membrane blebbing (5). In a lepidopteran cell line, SF-21, *rpr* expression induces cellular death with all the morphological and biochemical characteristics of apoptosis (6). RPR-induced apoptosis is associated with an increase in ceramide levels (5) and involves activation of one or more members of the caspase family of cysteine proteases (6, 7). In *Drosophila* embryos, *rpr* seems to be specifically expressed in cells that undergo apoptosis (3), and several death signals transcriptionally activate *rpr* expression (8). Although RPR was proposed to be related to death domain proteins (9, 10), recent evidence suggests that RPR is not a death domain homologue (6, 11, 12).

RPR-induced apoptosis can be blocked by two types of antiapoptotic proteins encoded by baculoviruses: P35 and inhibitors of apoptosis (IAPs). P35 is a broad-spectrum caspase inhibitor (13) which normally blocks apoptosis during baculovirus replication in SF-21 cells (14) but can also block RPR-induced apoptosis when ectopically expressed in *Drosophila* (4) and SF-21 cells (6). The founder members of the IAP family, baculovirus Op-IAP and Cp-IAP, were identified by their ability to substitute functionally for the baculovirus P35 (15–17), but they also block apoptosis induced by actinomycin D (17), RPR (6), or Doom (18) in SF-21 cells. Cp-IAP can partially block RPR-dependent apoptosis in *Drosophila* developing eyes (4), and Op-IAP partially blocks pro-ICE- and FADD-induced apoptosis in HeLa cells (19–21) and FADD-induced apoptosis in SF-21 cells (6). IAPs are characterized by the presence of two or three tandem baculovirus IAP repeat (BIR) motifs located at the amino-terminal and central portions of the protein, and most of them have a carboxyl-terminal RING finger motif. Op-IAP physically interacts through its BIR domain with Doom, an apoptosis-inducing member of the *mod* (*mdg4*) family (18).

Homologues of baculovirus IAPs have also been identified in eukaryotes. A *Drosophila* IAP homologue, D-IAP1, was identified in a screen for mutations that enhance the effect of RPR-induced apoptosis in the *Drosophila* developing eyes (4). D-IAP-2, a second *Drosophila* IAP, was identified by a search of the databases for sequences homologous to the known IAPs (4, 19, 20, 22). *Drosophila* IAPs block apoptosis induced by RPR in developing eyes (4), and D-IAP2 inhibits RPR-induced apoptosis in lepidopteran SF-21 cells (6). One of the four known human IAPs, NAIP, is linked to spinal muscular atrophy (SMA) which involves neuronal cell death (23). Two other mammalian IAPs, c-IAP1 and c-IAP2, are known to bind tumor necrosis factor receptor 2 (TNFR-2) associated factor 2 (TRAF-2) through their BIR domains (24). c-IAP1 is also a component of the TNFR-1 signaling complex (25) and may exert antiapoptotic activity by modifying signaling through TRAF-related pathways. Mammalian IAPs block apoptosis in several mammalian cell lines induced by a variety of stimuli (19, 20, 22).

Although baculovirus and *Drosophila* IAPs block RPR-induced apoptosis, the mechanism by which IAPs inhibit RPR-induced apoptosis is not known. In this study we investigated the possibility that these members of the IAP family physically interact with RPR. We also examined the effect of IAPs on stability and subcellular localization of RPR. *In vivo* binding studies demonstrated that both baculovirus and *Drosophila* IAPs physically interact with RPR and alter its subcellular localization. In addition, we found that RPR levels decline rapidly when expressed individually. Although this decline could be inhibited by coexpression with IAPs, caspases were not directly responsible for RPR disappearance.

MATERIALS AND METHODS

Cell Line. *Spodoptera frugiperda* (Lepidoptera: Noctuidae) IPLB-SF-21 (SF-21) cells were maintained in TC-100 medium (GIBCO/BRL) supplemented with 10% fetal bovine serum (Intergen; Purchase, NY) and 0.26% tryptose broth as previously described (26).

Expression Constructs. All the plasmids used in these studies are derived from pHSP70PLVI+CAT, a plasmid expressing the chloramphenicol acetyltransferase (*cat*) gene under the promoter of the *Drosophila* heat shock protein hsp70 (17). Plasmids expressing *rpr*-ORF, Op-*iap*, *p35*, D-*iap2*, or *cat*

The publication costs of this article were defrayed in part by page charge payment. This article must therefore be hereby marked "*advertisement*" in accordance with 18 U.S.C. §1734 solely to indicate this fact.

Abbreviations: IAP, inhibitor of apoptosis; BIR, baculovirus IAP repeat; HRP, horseradish peroxidase; DAPI, 4′,6-diamidino-2-phenylindole; CAT, chloramphenicol acetyltransferase; HA, hemagglutinin.

‡To whom reprint requests should be addressed. e-mail: miller@bscr.uga.edu.

(pHSP70PLVI+RPR-ORF, pHSOp-iapVI+, pHSp35VI+, pHSDIAP2VI+, or pHSP70PLVI+CAT) were previously described (6, 17). The plasmid expressing D-*iap1* was made by replacing *cat* from pHSP70PLVI+CAT with D-*iap1*. In rpr-Flag or rpr-Epi, *cat* is replaced with *rpr*-ORF C-terminally fused to either a FlagHis$_6$ tag or a hemagglutinin (HA).11His$_6$ tag; in Flag-Op-iap or Flag-cat, *cat* is replaced with Flag-epitope tag N-terminally fused to Op-*iap* or *cat*; in Epi-Op-iap, Epi-Op-BIR, Epi-Op-RING, Epi-D-iap2, Epi-D-iap1-BIR, Epi-p35, or Epi-cat, *cat* is replaced with HA.11-epitope tag N-terminally fused to Op-*iap*, Op-BIR, Op-RING, D-*iap2*, D-*iap1*-BIR, *p35*, or *cat*. Epi-Op-BIR construct encodes the amino acids 1–199, and Epi-Op-RING construct encodes the amino acids 198–268 of the 268 amino acid Op-*iap* ORF. Epi-D-iap1-BIR represents an epitope-tagged version of previously described construct (4). Site-specific mutagenesis was performed with the Transformer mutagenesis kit (CLONTECH) on rpr-ORF using selection primer (CAGCAGAGTCGCTAGCGATGTAAACGATGG) and mutagenic primer (GCATTCTACATACCCGCTCAGGCGACTCTG) to generate rpr-D9A. All the Flag- and HA.11-epitope-tagged constructs were tested in several apoptotic assays and were functionally identical to their nontagged counterparts.

***In Vivo* Binding Assay.** SF-21 cells (10^6 per 60-mm tissue culture dish) transiently transfected by Lipofectin-mediated transfection (GIBCO/BRL) included 5 μg of each of the indicated plasmids and 2 μg of pHSp35VI+ to prevent apoptosis and thus maintain protein expression. The cells were heat shocked 20 h after transfection for 30 min at 42°C as described (17). At 3 h after heat shock, the cells were harvested and pelleted at 500 $\times$ *g*. Cells were lysed in 80 μl of NP-40 lysis buffer (50 mM Tris·HCl, pH 8.0/150 mM NaCl/1.0% Nonidet P-40/1 mM dithiothreitol/1 mM phenylmethylsulfonyl fluoride) at 4°C for 30 min with agitation. The lysate was centrifuged at 12,000 $\times$ *g* for 5 min and an aliquot of the supernatant (10 μl) was reserved for immunoblot analysis of the total lysate. Ten microliters of anti-Flag affinity resin (Eastman) was incubated with the remainder of the supernatant for 4 h at 4°C with agitation. The resin was washed five times in 500 μl of NP-40 lysis buffer. Aliquots of the total cell lysate and precipitates were separated by SDS/15% polyacrylamide gel electrophoresis (PAGE) and transferred to Immobilon-P membranes (Millipore). HA-epitope-tagged constructs were detected with rabbit anti-HA.11 polyclonal antiserum (Berkeley Antibody, Richmond, CA) and goat anti-rabbit IgG-horseradish peroxidase (HRP) conjugate (Promega) (precipitates) or with mouse HA.11 monoclonal antibody and rabbit anti-mouse IgG HRP conjugate (Amersham) (aliquots of the total cell lysates). Flag-tagged constructs were detected with anti-Flag M2 monoclonal antibody and rabbit anti-mouse IgG HRP conjugate (Amersham).

Immunofluorescence Microscopy. SF-21 cells (10^5 cells per well in 4-well Lab-Tek Chamber Slides (Nunc) were transfected and heat shocked as previously described (6). Eighty minutes or 4 h after heat shock, cells were washed once in PBS, pH 6.2, fixed in 3.7% formaldehyde/PBS, pH 6.2, and washed three times in PBS, pH 7.2. Cells were permeabilized in 0.5% Triton X-100/PBS, pH 7.2, washed three times in PBS, pH 7.2, and incubated in blocking buffer (5% BSA/10% goat serum/PBS, pH 7.2). Flag-tagged constructs were detected with mouse M2 anti-Flag monoclonal antibody and lissamine rhodamine-conjugated goat anti-mouse IgG + IgM antibody (Jackson ImmunoResearch). HA-epitope-tagged constructs were detected with rabbit anti-HA.11 polyclonal antiserum and fluorescein isothiocyanate-conjugated goat anti-rabbit IgG antibody (Sigma). Determination of the location and condition of nuclei was accomplished by staining with 4′,6-diamidino-2-phenylindole (DAPI; Sigma). Cells were examined and photographed using confocal microscopy.

Immunoblot Analysis. SF-21 cells were transfected and heat shocked as described (6). The cells were harvested 80 min, 4 h, or 8 h after heat shock and lysed in SDS sample buffer (6). Proteins were separated by SDS/15% PAGE and transferred to membranes which were then probed with polyclonal anti-RPR antiserum (obtained from G. J. Pronk, Chiron) and goat anti-rabbit IgG HRP conjugate, or anti-Flag M2 monoclonal antibody and rabbit anti-mouse IgG HRP conjugate.

RESULTS AND DISCUSSION

To investigate the possibility that baculovirus and *Drosophila* IAPs physically interact with RPR, we transiently coexpressed RPR-Flag, a fusion of RPR and a Flag epitope tag, with HA-epitope-tagged versions of a baculovirus IAP, Epi-Op-IAP, or a *Drosophila* IAP, Epi-D-IAP2, and determined if antibodies to the RPR-Flag protein could coimmunoprecipitate the IAP fusion proteins. As controls, we tested HA-tagged versions of the baculovirus P35 (Epi-P35) and bacterial CAT (Epi-CAT) proteins. We found that both Op-IAP and D-IAP2 coprecipitated with RPR (Fig. 1*A*, lanes 1 and 6), but P35 and CAT did not (Fig. 1*A*, lanes 2 and 8) even though they were efficiently expressed (Fig. 1*B*, lanes 2 and 8). In a reciprocal experiment, Flag-tagged Op-IAP (Flag-Op-IAP) specifically coprecipitated with a HA-epitope-tagged RPR (RPR-Epi) (data not shown).

To determine which portion of Op-IAP possessed RPR binding activity, we tested the ability of HA-tagged BIR and RING finger domains to individually bind RPR-Flag. The Epi-Op-BIR protein coimmunoprecipitated with RPR-Flag (Fig. 1*A*, lane 3), but the Epi-Op-RING protein did not coimmunoprecipitate (Fig. 1*A*, lane 4) even though it was efficiently expressed (Fig. 1*B*, lane 4). Expression of the Flag-tagged and HA-tagged constructs in the cell lysates were confirmed for all transfections (Fig. 1 *B* and *C*). The BIR region of D-IAP1, which has been shown to have antiapoptotic activity (4), inhibited RPR-induced apoptosis in SF-21 cells and also specifically coprecipitated with RPR (data not shown). Therefore, baculovirus and *Drosophila* IAPs bind to RPR, and the region encompassing their BIR motifs is necessary for this protein–protein interaction.

The ability of IAPs to bind RPR suggested that IAPs and RPR should localize to the same subcellular location when coexpressed. To verify this, SF-21 cells were transfected with RPR-Flag in the presence or absence of HA-tagged IAPs. In the absence of inhibitors of apoptosis, RPR was observed at 80 min after induction and localized predominantly to the cytoplasm of the cells (Fig. 2*D*). By 4 h after induction, there was no evidence of RPR within the cells (Fig. 2*E*). Furthermore, there was no evidence of the formation of aggregates of RPR, suggesting that RPR disappearance is probably due to proteolytic degradation. Expression of RPR in the absence of inhibitors of apoptosis caused nuclear condensation and fragmentation in transfected cells observed by DAPI staining (Fig. 2*F*). SF-21 cells expressing CAT served as a negative control (Fig. 2 *A–C*).

When coexpressed with RPR, P35 inhibited RPR-induced nuclear condensation and fragmentation (Fig. 2*I*), and RPR was observed in the cytoplasm of transfected cells at 80 min and 4 h after induction (Fig. 2 *G* and *H*). Op-IAP also blocked both RPR-induced nuclear condensation and fragmentation (Fig. 2*M*) and the rapid disappearance of RPR, but in this case, RPR displayed a punctate perinuclear localization beginning at 80 min after induction (Fig. 2*J*) and more pronounced at 4 h after induction (Fig. 2*K*) which coincided with the subcellular localization of Op-IAP (Fig. 2*L*). The same punctate perinuclear pattern of subcellular localization was observed for Op-IAP in the absence of RPR at 4 h after induction (Fig. 2*N*). Furthermore, reversing the epitope tags on RPR and Op-IAP

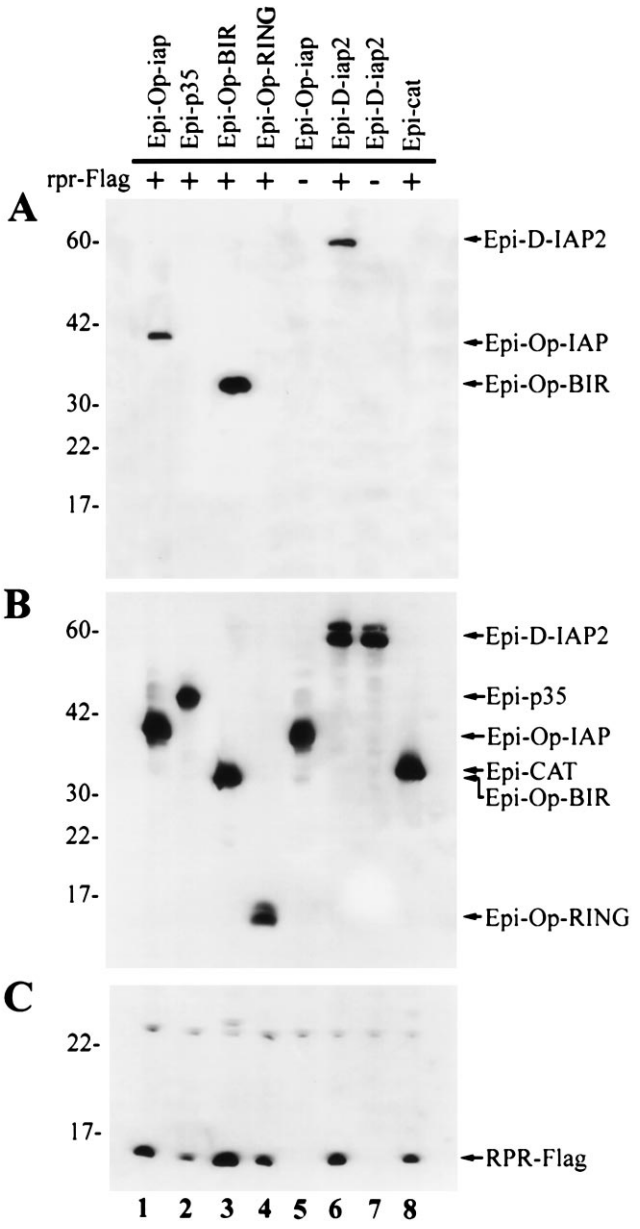

FIG. 1. IAPs physically interact with RPR. (*A*) SF-21 cells were transiently transfected with plasmids expressing RPR-Flag and indicated HA-epitope-tagged (Epi) genes. At 3 h after heat shock, aliquots of cell lysates were immunoprecipitated with the M2 anti-Flag monoclonal antibody resin. Coprecipitated HA-epitope-tagged constructs were detected by immunoblot analysis with the rabbit anti-HA.11 polyclonal antiserum. The positions of the HA-epitope-tagged proteins are indicated by arrows on the right. Molecular mass markers (in kDa) are shown on the left. (*B*) Expression of the HA-epitope-tagged proteins was confirmed by immunoblot analysis with the mouse HA.11 monoclonal antibody of aliquots of the total cell lysates from *A*. (*C*) Expression of RPR-Flag was confirmed by immunoblot analysis with the M2 anti-Flag antibody of aliquots of the total cell lysates from *A*. The position of RPR-Flag is indicated by the arrow on the right.

resulted in the same subcellular localization pattern when coexpressed or expressed individually (data not shown).

D-IAP2 displayed a staining pattern similar to that of Op-IAP in the absence of RPR (Fig. 2*O*), although D-IAP2 staining was not as punctate as Op-IAP staining (Fig. 2, compare *N* and *O*). In the presence of RPR, D-IAP2 inhibited RPR-induced nuclear condensation and fragmentation (Fig. 2*R*), inhibited the rapid disappearance of RPR, and showed overlapping subcellular localization (Fig. 2 *P* and *Q*). Colocalization of RPR and D-IAP2 was not as evident as for RPR and Op-IAP, perhaps because D-IAP2 displayed slightly more diffuse staining compared with Op-IAP (Fig. 2, compare *N* and *O*).

Consistent with microscopic observations that RPR disappears 4 h after induction, we found that RPR was easily detected by Western blot analysis at 80 min after induction, but was undetectable by 4 h or 8 h after induction (Fig. 3*A*, lanes 1–3). This finding prompted us to investigate the fate of RPR under conditions in which apoptosis was induced by RPR compared with conditions in which RPR-induced apoptosis was blocked by Op-IAP. When coexpressed with Op-IAP, RPR accumulated during the 8-h period after induction, and additional bands of higher molecular mass were observed concomitantly (Fig. 3*A*, lanes 4–6). Because coexpression of Op-IAP blocked RPR-induced apoptosis, we tested whether coexpression of RPR with another apoptosis inhibitor, baculovirus P35, would affect RPR levels. Despite its ability to block RPR-induced apoptosis as efficiently as Op-IAP, P35 delayed but was unable to completely inhibit the disappearance of RPR, and the higher molecular mass bands were not observed (Fig. 3*A*, lanes 7–9).

The inability of P35 to block RPR disappearance suggested that RPR was not proteolytically degraded by a member of the caspase family of proteases, which cleave their substrates specifically after aspartate residues. To confirm this, we mutated the sole aspartate of RPR to alanine. This mutant, RPR D9A, efficiently induced apoptosis (data not shown) and behaved in the same manner as RPR by Western blot analysis (Fig. 3*B*), confirming that disappearance of RPR is not due to the direct proteolytic activity of the caspases.

We also observed that RPR-Flag displayed the same protein profile as untagged RPR when detected with the anti-Flag antibody. Thus, the disappearance of RPR is not due to the masking of an epitope. Additional bands of higher molecular mass were also detected by the anti-Flag antibody and are thus RPR related (Fig. 3*C*). We have not determined the nature of the higher molecular mass bands visible in lanes 5 and 6 of Fig. 2 *A–C*. Although the sizes of the two major new bands, approximately 13 and 26 kDa, are consistent with the size of dimers and tetramers of RPR, the products may also be due to post-translational modification such as ubiquitination. We also generated a RPR fusion consisting of HA.11, His_6, and CAT C-terminally fused to RPR and analyzed it in the same way as shown in Fig. 3. Additional bands of higher molecular mass that were detected by the anti-HA antibody represented increments of 7–8 kDa (data not shown), which is consistent with the ubiquitin hypothesis.

As a control, we investigated the stability of a control protein, Flag-CAT, under the same conditions as in Fig. 3 *A*, *B*, or *C*. Under conditions when RPR induced apoptosis, the amount of Flag-CAT decreased approximately 5-fold by 8 h after induction, in contrast to RPR, which completely disappeared by 4 h after induction (Fig. 3*D*, lanes 1–3). Furthermore, while P35 only delayed and Op-IAP completely blocked the disappearance of RPR, P35 and Op-IAP both equally blocked the decline in Flag-CAT levels (Fig. 3*D*, lanes 4–9). Thus, the 5-fold decline in Flag-CAT levels is apparently due to caspase activation during RPR-induced apoptosis. In additional experiments we established that coexpression of either D-IAP1 or D-IAP2 had the same effect on the levels of Flag-RPR as Op-IAP, and that HA-tagged RPR and CAT produced the same result in immunoblot analysis as Flag-tagged constructs (data not shown).

Concluding Remarks. We have found that baculovirus Op-IAP and *Drosophila* IAPs physically associate with *Drosophila* RPR. The region encompassing their BIR motifs is necessary and sufficient for this interaction. Our findings are consistent with *in vivo* data as mutations in *thread*, which encodes D-IAP1, enhance RPR-induced cell death in *Drosophila* developing eyes (4). RPR is the third protein reported

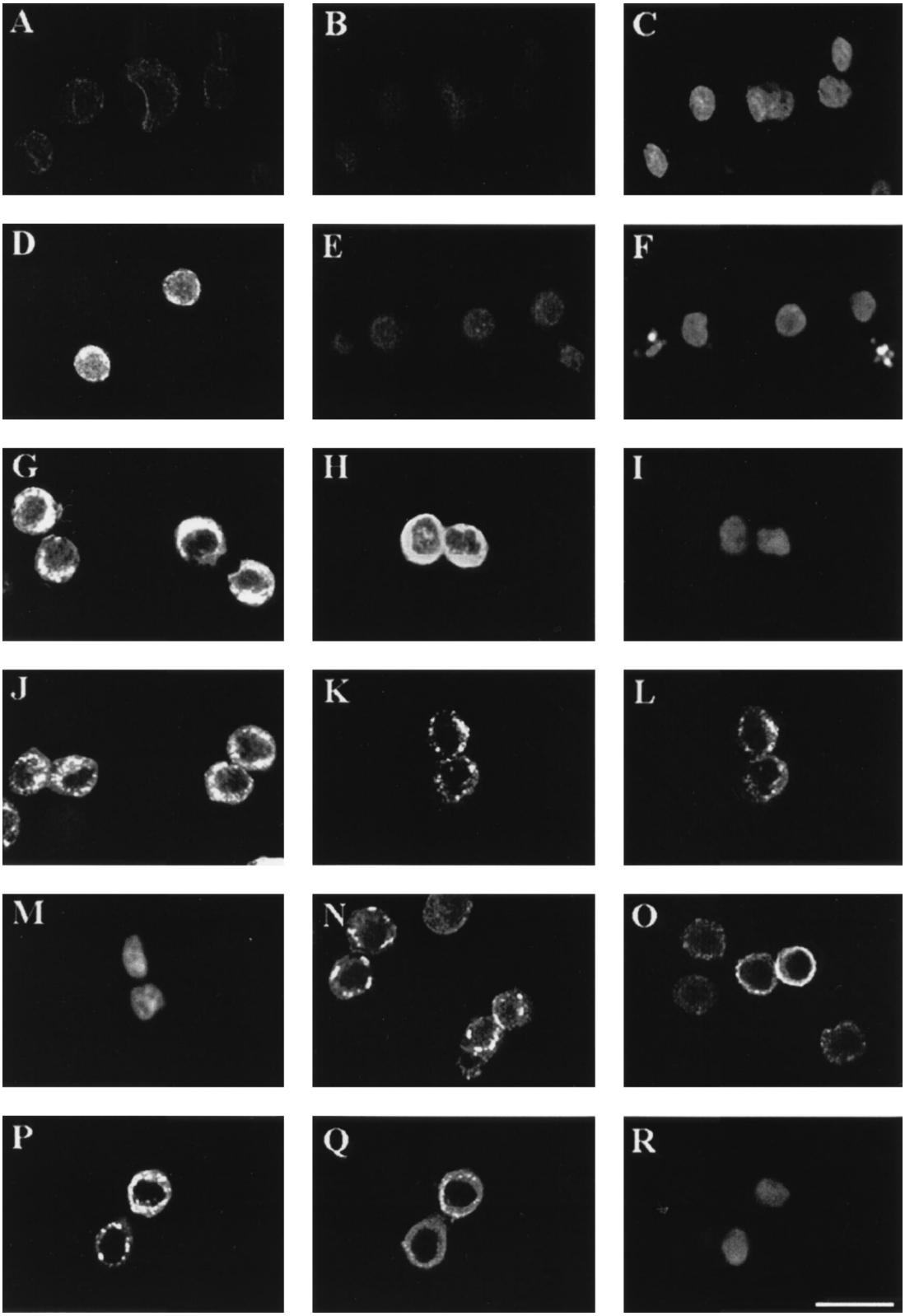

FIG. 2. Colocalization of IAPs and RPR. SF-21 cells were transiently transfected with plasmids expressing CAT (*A–C*; all taken from the same field of cells), RPR-Flag and CAT (*D–F*; *E* and *F* are the same field), RPR-Flag and P35 (*G–I*; *H* and *I* are the same field), RPR-Flag and Epi-Op-IAP (*J–M*; *K–M* are the same field), Epi-Op-IAP (*N*), Epi-D-IAP2 (*O*), or RPR-Flag and Epi-D-IAP2 (*P–R*; all from the same field). At 80 min (*D*, *G*, and *J*) or 4 h (*A–C, E, F, H, I*, and *K–R*) after heat shock, cells were fixed with formaldehyde, permeabilized, and analyzed by indirect immunofluorescence. RPR-Flag was visualized with mouse M2 anti-Flag monoclonal antibody and lissamine rhodamine-conjugated goat anti-mouse IgG + IgM antibody, (*D, E, G, H, J, K*, and *P*). HA-epitope-tagged proteins were visualized with rabbit anti-HA.11 polyclonal antiserum and fluorescein isothiocyanate-conjugated goat anti-rabbit IgG antibody, (*L, N, O*, and *Q*). Nuclei were visualized by costaining with DAPI (*C, F, I, M*, and *R*). CAT-transfected cells were probed with rabbit anti-HA.11 polyclonal antiserum and fluorescein isothiocyanate-conjugated goat anti-rabbit IgG antibody (*A*), mouse M2 anti-Flag monoclonal antibody and lissamine rhodamine-conjugated goat anti-mouse IgG + IgM antibody (*B*), or stained with DAPI (*C*). (Scale bar equals 25 μm.)

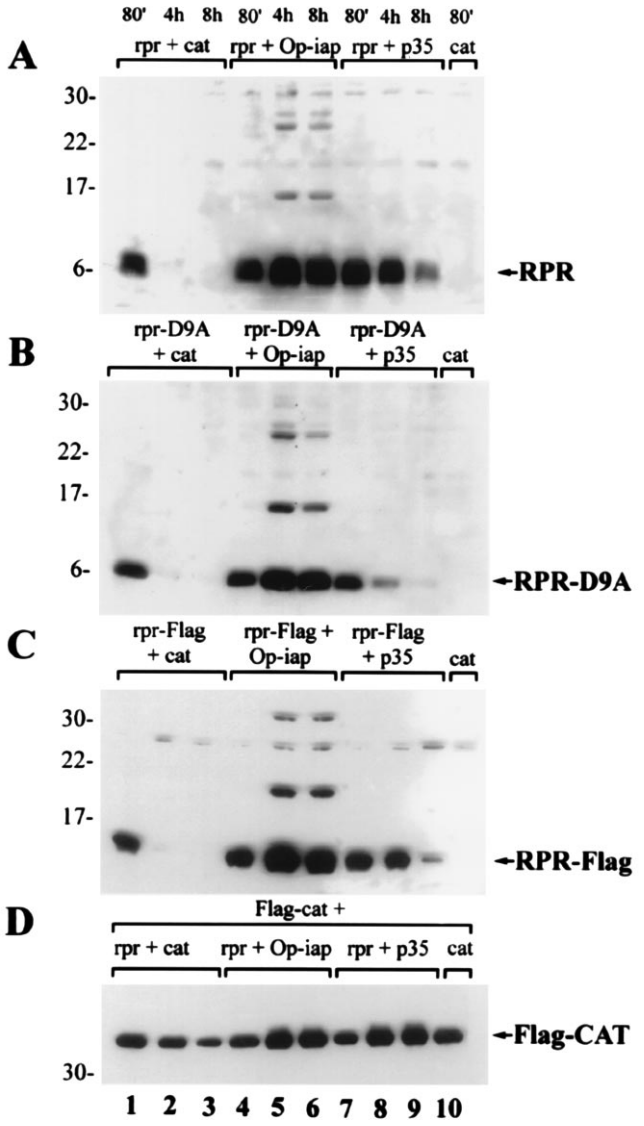

FIG. 3. Kinetics of disappearance of RPR. SF-21 cells were transiently transfected with plasmids expressing combinations of genes indicated above the lanes of each panel and harvested 80 min (lanes 1, 4, 7, and 10), 4 h (lanes 2, 5, and 8) or 8 h (lanes 3, 6, and 9) after heat shock. Immunoblot analysis was done with the anti-RPR antiserum (*A* and *B*) or the M2 anti-Flag antibody (*C* and *D*), and the arrows at the right point to the major expected product for each of the expressed genes. Molecular mass markers (in kDa) are shown at the left.

to interact with IAPs but the only one of these three proteins that has been clearly assigned a role in apoptosis genetically. Evidence that mammalian c-IAPs have a role in apoptosis is based on their biochemical association with TRAF-2, which is thought to influence signal transduction from both TNFR-1 and TNFR-2. *Drosophila* Doom has been found both to associate with baculovirus IAPs and to induce apoptosis upon over-expression in SF-21 cells. Although the common property of these proteins is their ability to bind the BIR motif region of IAPs, they share no obvious sequence similarity. The ability of IAPs to block apoptosis induced by a variety of different signals and their ability to interact physically with multiple inducers of apoptosis suggests that IAPs serve as central control points for sensing and blocking cell death signals transduced through a number of different pathways.

Binding of RPR to Op-IAP or D-IAP2 results in its localization to the same cellular location as IAPs. This localization is IAP-directed because RPR localizes diffusely within the cytoplasm in the absence of IAPs (e.g., when expressed with P35, which does not bind RPR but which delays its disappearance). Over-expression of IAPs in SF-21 cells results in their localization to punctate regions of the cytoplasm which, in these studies, appear to be perinuclear in their subcellular location. Op-IAP has been reported to be cytoplasmic as well as membrane-associated (18, 27). Mammalian c-IAPs were found associated with TNFR-2, whereas Op-IAP relocalized to the nucleus when bound to Doom. Thus, the cellular location of IAPs may depend on their binding partners. The significance of the relocalization of RPR to the location of the IAPs in SF-21 cells remains to be established. However, because IAPs do not alter their location upon infection by baculoviruses or upon UV irradiation (27), it is likely that apoptosis induced by these signals does not involve a Doom-like inducer but may involve a RPR-like inducer.

We have found that the levels of RPR decline rapidly following induction in SF-21 cells; the stability of RPR in *Drosophila* cells has not yet been assessed. The rapid decline in RPR is not due to cleavage by caspases, which are known to be activated during RPR-induced apoptosis, because mutation of the single aspartate residue of RPR does not alter either its ability to induce apoptosis or its rate of disappearance. However, induction of caspases does in some way reduce RPR levels, because coexpression of RPR with P35 delays RPR disappearance after induction. Coexpression of RPR with IAPs results in accumulation of RPR to high levels and the appearance of higher molecular mass forms of RPR. The nature of these larger forms of RPR is not known, but their molecular masses suggest the possibility of a post-translational modification such as ubiquitination. Whether IAP binding targets RPR for ubiquitin-mediated degradation or merely stabilizes these transient forms of RPR is not yet known. The rapid turnover of apoptotic inducers such as RPR would allow precision control of the concentration of the inducer and finer tuning of the cellular environment.

Physical association of RPR with IAPs provides a mechanism by which IAPs can inhibit RPR-induced apoptosis. IAPs may physically block RPR's access to effector proteins through this interaction. Alternately, RPR binding to IAPs may displace IAPs from binding to effector proteins. A third possibility is that by redirecting RPR to a different subcellular location, IAPs may block RPR's access to an effector or alter its function in another way. We favor the model that IAPs serve as sensors of multiple apoptotic induction signals and, by binding, serve as a buffer to the induction of apoptosis; when the levels of inducers rise above the threshold determined by IAP levels, apoptosis ensues.

We thank B. A. Hay (California Institute of Technology) for the D-*iap*1 and D-*iap*1 BIR cDNA, G. J. Pronk (Chiron) for the anti-RPR antiserum, S. Seshagiri for the construction of Epi-*p35* and helpful discussions, and C. V. C. Glover III, K. White, and J. M. Hardwick for helpful comments. This work was supported in part by Public Health Service Grant AI38262 from the National Institute of Allergy and Infectious Disease to L.K.M.

1. Steller, H. (1995) *Science* **267,** 1445–1449.
2. Thompson, C. B. (1995) *Science* **267,** 1456–1462.
3. White, K., Grether, M. E., Abrams, J. M., Young, L., Farrell, K. & Steller, H. (1994) *Science* **264,** 677–683.
4. Hay, B. A., Wassarman, D. A. & Rubin, G. M. (1995) *Cell* **83,** 1253–1262.
5. Pronk, G. J., Ramer, K., Amiri, P. & Williams, L. T. (1996) *Science* **271,** 808–810.
6. Vucic, D., Seshagiri, S. & Miller, L. K. (1997) *Mol. Cell. Biol.* **17,** 667–676.

7. White, K., Tahaoglu, E. & Steller, H. (1996) *Science* **271,** 805–807.
8. Nordstrom, W., Chen, P., Steller, H. & Abrams, J. M. (1996) *Dev. Biol.* **180,** 213–226.
9. Golstein, P., Marguet, D. & Depraetere, V. (1995) *Cell* **81,** 185–186.
10. Cleveland, J. L. & Ihle, J. N. (1995) *Cell* **81,** 479–482.
11. Chen, P., Lee, P., Otto, L. & Abrams, J. (1996) *J. Biol. Chem.* **271,** 25735–25737.
12. Huang, B., Eberstadt, M., Olejniczak, E. T., Meadows, R. P. & Fesik, S. W. (1996) *Nature (London)* **384,** 638–641.
13. Bump, N. J., Hackett, M., Hugunin, M., Seshagiri, S., Brady, K., Chen, P., Ferenz, C., Franklin, S., Ghayur, T., Li, P., Licari, P., Mankovich, J., Shi, L., Greenberg, A. H., Miller, L. K. & Wong, W. W. (1995) *Science* **269,** 1885–1888.
14. Clem, R. J., Fechheimer, M. & Miller, L. K. (1991) *Science* **254,** 1388–1390.
15. Birnbaum, M. J., Clem, R. J. & Miller, L. K. (1994) *J. Virol.* **68,** 2521–2528.
16. Crook, N. E., Clem, R. J. & Miller, L. K. (1993) *J. Virol.* **67,** 2168–2174.
17. Clem, R. J. & Miller, L. K. (1994) *Mol. Cell. Biol.* **14,** 5212–5222.
18. Harvey, A. J., Bidwai, A. P. & Miller, L. K. (1997) *Mol. Cell. Biol.* **17,** 2835–2843.
19. Duckett, C. S., Nava, V. E., Gedrich, R. W., Clem, R. J., Van Dongen, J. L., Gilfillan, M. C., Shiels, H., Hardwick, J. M. & Thompson, C. B. (1996) *EMBO J.* **15,** 2685–2694.
20. Uren, A. G., Pakusch, M., Hawkins, C. J., Puls, K. L. & Vaux, D. L. (1996) *Proc. Natl. Acad. Sci. USA* **93,** 4974–4978.
21. Hawkins, C. J., Uren, A. G., Hacker, G., Medcalf, R. L. & Vaux, D. L. (1996) *Proc. Natl. Acad. Sci. USA* **93,** 13786–13790.
22. Liston, P., Roy, N., Tamai, K., Lefebvre, C., Baird, S., Cherton-Horvat, G., Farahani, R., McLean, M., Ikeda, J. E., MacKenzie, A. & Korneluk, R. G. (1996) *Nature (London)* **379,** 349–353.
23. Roy, N., Mahadevan, M. S., McLean, M., Shutler, G., Yaraghi, Z., *et al.* (1995) *Cell* **80,** 167–178.
24. Rothe, M., Pan, M. G., Henzel, W. J., Ayres, T. M. & Goeddel, D. V. (1995) *Cell* **83,** 1243–1252.
25. Shu, H., Takeuchi, M. & Goeddel, D. V. (1996) *Immunology* **93,** 13973–13978.
26. O'Reilly, D. R., Miller, L. K. & Luckow, V. A. (1992) *Baculovirus Expression Vectors: A Laboratory Manual* (Freeman, New York).
27. Manji, G. A., Hozak, R. R., LaCount, D. J. & Friesen, P. D. (1997) *J. Virol.* **71,** 4509–4516.